

# Primary evaluation the effects of *Boesenbergia pandurata* ethanol extract on etoposide-induced senescence in fibroblasts

Phuc Hong Vo<sup>1,2</sup>, Nghia Minh Do<sup>1,2</sup>, Sinh Truong Nguyen<sup>1,2,\*</sup>

## ABSTRACT

**Introduction:** Cellular senescence is an extensively researched issue aimed at influencing the aging process. A novel research direction involves studying the potential of plant extracts on this process. *Boesenbergia pandurata* (Roxb.) Schltr, also known as *Boesenbergia rotunda* (L.) Mansf, is a herb with significant potential for research into its effects on aging. Furthermore, it is crucial to study cellular senescence models to accurately assess the impact of various agents on the aging process. **Methods:** In this study, the ethanol extract of *Boesenbergia pandurata* (Roxb.) Schltr was evaluated for its potential effects on certain characteristics of senescent fibroblasts derived from foreskin, which were induced by etoposide. The cells were treated with 20  $\mu\text{M}$  etoposide for 48 hours to induce senescence. **Results:** The study demonstrated that treating fibroblasts with 20  $\mu\text{M}$  etoposide for 48 hours induces senescence characteristics. Additionally, administering the ethanol extract of *Boesenbergia pandurata* at a concentration of 15  $\mu\text{g/ml}$  ameliorated several features of senescence in fibroblasts. The treatment resulted in a 27% reduction in cell size ( $p < 0.05$ ), a 1.2-fold decrease in SA- $\beta$ -Galactosidase enzyme activity ( $p < 0.0001$ ), and reduced gene expression of p16, p21, and p53. **Conclusion:** We established a senescent fibroblast model using 20  $\mu\text{M}$  etoposide and demonstrated that the finger root extract at 15  $\mu\text{g/ml}$  improved various senescence-related cellular characteristics, suggesting its potential as an anti-aging agent.

**Key words:** Boesenbergia pandurata, Etoposide, Senescent fibroblast, SA- $\beta$ -gal

## INTRODUCTION

The previous study determined the characteristics as the hallmark of aging at the body level<sup>1,2</sup>. One of the hallmarks of aging, cellular senescence, is carefully researched and analyzed in terms of understanding the mechanism of aging<sup>1,3</sup>. The senescence cell model plays an important role in the development of anti-aging therapies<sup>4,5</sup>. Key aging processes include chronic sterile low-grade inflammation, macromolecular and organelle dysfunction, stem and progenitor cell impairment, and cellular senescence. These processes are not only central to the development of age-related phenotypes but also frequently manifest in the pathological sites of age-associated chronic diseases<sup>6</sup>. According to the unitary theory of fundamental aging processes, intervening in one primary aging mechanism may have a cascading effect on others due to their relationships. The buildup of senescent cells, associated with chronic diseases and age-related health issues, underscores the potential of targeting these cells as a comprehensive approach to address whole-body aging<sup>7</sup>.

Cellular senescence is a complex process in which relevant cellular changes and molecular, morphological changes, including nonproliferation and interaction

with stimulated cell division<sup>8</sup>. When cells become senescent, they undergo fundamental changes and express specific characteristics that distinguish them from normal cells<sup>9</sup>. However, until now, there is no confirmation to determine the aging level of cells *in vitro*. Thus, the assessment relying on the characteristics that senescent cells express is considered a marker that determines cellular senescence.

The hallmark of senescent cells is the decreased proliferation of cells. Cell morphology also undergoes alterations during the aging process. Senescent cells become larger and more flattened, acquiring a "fried egg" appearance. Furthermore, in certain cell types such as fibroblasts, senescence is characterized by increased nuclear and nucleolar size, elevated lysosome production, and enhanced development of the Golgi apparatus<sup>10</sup>. Senescence-associated  $\beta$ -galactosidase (SA- $\beta$ -gal) activity serves as a commonly employed marker for identifying senescent cells within cell populations and can be histochemically detected at pH 6 *in vitro*. The observed accumulation of SA- $\beta$ -gal in senescent cells is primarily attributable to an increase in both lysosome number and activity, along with contributions from oxidative stress and alterations in cellular signaling pathways<sup>11-13</sup>. At the molecular

<sup>1</sup>Stem Cell Institute, University of Science Ho Chi Minh City, Ho Chi Minh City, Viet Nam

<sup>2</sup>Viet Nam National University Ho Chi Minh City, Ho Chi Minh City, Viet Nam

### Correspondence

**Sinh Truong Nguyen**, Stem Cell Institute, University of Science Ho Chi Minh City, Ho Chi Minh City, Viet Nam  
Viet Nam National University Ho Chi Minh City, Ho Chi Minh City, Viet Nam  
Email: sinhnghuyen@sci.edu.vn

### History

- Received: Oct 09, 2024
- Accepted: Nov 20, 2024
- Published Online: Nov 30, 2024

DOI : 10.15419/bmrat.v11i11.933



### Copyright

© Biomedpress. This is an open-access article distributed under the terms of the Creative Commons Attribution 4.0 International license.



**Cite this article :** Vo P H, N M D, Nguyen S T. Primary evaluation the effects of *Boesenbergia pandurata* ethanol extract on etoposide-induced senescence in fibroblasts. *Biomed. Res. Ther.* 2024; 11(11):6869-6882.

level, senescent cells often exhibit cell cycle arrest and regulatory factors such as p16INK4A, p21CIP1, and p53 are commonly utilized to detect these senescent cells<sup>14</sup>. Additionally, senescent cells secrete a variety of pro-inflammatory cytokines, chemokines, growth factors, and matrix metalloproteinases (MMPs), collectively known as the senescence-associated secretory phenotype (SASP)<sup>4,15</sup>. This secretion profile can be leveraged as a strategy for identifying senescent cells. Recently, there have been many methods to generate senescent cell models such as UVB and chemical stimuli. Among these, etoposide is the preventive cancer agent found to cause cell aging during use<sup>16</sup>. Cell senescence was induced by low doses of etoposide, while apoptosis was activated at higher doses<sup>17</sup>. Therefore, etoposide is used as an inducer of cell senescence.

*Boesenbergia pandurata* (Roxb.) Schltr, also known as *Boesenbergia rotunda* (L.) Mansf, is a plant species native to tropical countries. *Boesenbergia pandurata* rhizomes have been used for food and folk medicine<sup>18,19</sup>. *Boesenbergia pandurata* exhibits significant aesthetic potential, particularly in aging research because of its antioxidant potential. Research on natural substances that can delay skin aging has been the object of increasing interest in the last few years. To investigate the potential benefits of *Boesenbergia pandurata*, we developed a senescent fibroblast model and conducted a preliminary evaluation of the effects of this rhizome extract on the senescence process in young human foreskin fibroblasts, induced by various concentrations of etoposide.

## METHODS

### Preparation of *Boesenbergia Pandurata* Extract

The rhizomes of *Boesenbergia pandurata* were harvested from the Southwest region of Viet Nam and subsequently identified at the Southern Institute of Ecology, Viet Nam. Fresh rhizomes were thoroughly cleaned and ground before undergoing solvent extraction. Specifically, 100 grams of the ground rhizomes were subjected to extraction with 500 mL of absolute ethanol for 72 hours using the maceration technique. The resultant extract was then filtered and subjected to freeze-drying at -40°C. The resulting dry extract was reconstituted in absolute ethanol to achieve a final concentration of 200 mg/mL. This stock solution was stored at 4°C for subsequent experimental procedures.

### Cell Lines

The foreskin fibroblast cell line was provided by the Stem Cell Institute, University of Science - Viet Nam National University, Ho Chi Minh City, Viet Nam. These cells were cultured in D'MEM/F12 (Lonza, UK), supplemented with 10% FBS (Gibco, UK) and 1% antibiotic (Gibco, UK) under 5% CO<sub>2</sub> and 37°C.

### Cytotoxicity Assay

Human fibroblasts (2.5 x 10<sup>4</sup> cells/mL) were seeded in a 96-well plate in 100 μL of culture medium. After 24 hours, hFs were treated with etoposide (Abcam, UK) at concentrations of 240 μM, 120 μM, 60 μM, 30 μM, 15 μM, 7.5 μM, 3.75 μM, 1.875 μM, 0.9375 μM and control for 48 hours. Cells were evaluated for their viability by staining with Alamar Blue for 1 hour and reading the measurements using a DTX 880 multimode reader (Beckman Coulter, CA).

For testing the *Boesenbergia pandurata* extract (BPE) potential, human fibroblasts (hFs) (2.5 x 10<sup>4</sup> cells/mL) were seeded in a 96-well plate in 100 μL of culture medium. After 24 hours, hFs were treated with BPE at concentrations of 2000 μg/ml, 1000 μg/ml, 500 μg/ml, 250 μg/ml, 125 μg/ml, 60 μg/ml, 30 μg/ml, 15 μg/ml, 7.5 μg/ml and control for 48 hours. Cells were evaluated for their viability by staining with Alamar Blue for 1 hour and reading the measurements using a DTX 880 multimode reader (Beckman Coulter, CA).

### Cell Size Assay

Human fibroblasts (5 x 10<sup>3</sup> cells/well) were cultured in a 48-well plate in 200 μL of culture medium. After 24 hours, the cells were treated with etoposide at concentrations of 10 μM, 20 μM, 30 μM and control for 48 hours. The suspension cells were observed under 40X magnification. Three ROIs (Regions of Interest) per well were captured under a light microscope to measure their diameter using AxioVision 4.8 software (Zeiss, Germany).

For the BPE testing, hFs (5 x 10<sup>3</sup> cells/well) were cultured in a 48-well plate in 200 μL of culture medium. After 24 hours, the cells were treated with 20 μM etoposide to make a senescent fibroblast model for 48 hours. After that, the cells were washed with 200 μL PBS-. The experimental groups were treated with the BP extract at concentrations of 60 μg/ml, 30 μg/ml, 15 μg/ml. The senescent group and the control group were cultured with culture medium. After 48 hours, the suspension cells were observed under 40X magnification. Three ROIs per well were captured under a light microscope to measure their diameter using AxioVision 4.8 software (Zeiss, Germany).

### SA- $\beta$ -Galactosidase Staining Assay

Human fibroblasts ( $5 \times 10^3$  cells/well) were seeded in a 48-well plate in 200  $\mu$ L of culture medium. After 24 hours, the cells were treated with etoposide at 10  $\mu$ M, 20  $\mu$ M, 30  $\mu$ M and control for 48 hours. Afterward, the cells were stained following the protocol of the beta Galactosidase Staining Kit (ab102534) (Abcam, UK). Three ROIs per well were captured under a light microscope. The  $\beta$ -galactosidase-positive cell ratio was then calculated by dividing the total number of  $\beta$ -galactosidase-positive cells by the total number of cells.

For the BPE testing, human fibroblasts ( $5 \times 10^3$  cells/well) were cultured in a 48-well plate in 200  $\mu$ L of culture medium. After 24 hours, the cells were treated with 20  $\mu$ M etoposide to make a senescent fibroblast model for 48 hours. After that, the cells were washed with 200  $\mu$ L PBS<sup>-</sup>. The experimental groups were treated with the BPE at concentrations of 60  $\mu$ g/ml, 30  $\mu$ g/ml, 15  $\mu$ g/ml. The senescent group and the control group were cultured with culture medium. After 48 hours, cells were stained according to the beta Galactosidase Staining Kit protocol (ab102534) (Abcam, UK). Three ROIs per well were captured under a light microscope. The  $\beta$ -galactosidase-positive cell ratio was then calculated by dividing the total number of  $\beta$ -galactosidase-positive cells by the total number of cells.

### RNA Isolation

Human fibroblasts ( $2 \times 10^5$  cells/mL) were seeded in a 6-well plate in 1 mL of culture medium. After 24 hours, the cells were treated with etoposide at 10  $\mu$ M, 20  $\mu$ M, 30  $\mu$ M and control for 48 hours. After that, the total RNA from the fibroblasts was extracted using the Easy-Blue Total RNA Extraction Kit (iNtRON Biotechnology).

For the BPE testing, human fibroblasts ( $5 \times 10^3$  cells/well) were cultured in a 48-well plate in 200  $\mu$ L of culture medium. After 24 hours, the cells were treated with 20  $\mu$ M etoposide to make a senescent fibroblast model for 48 hours. After that, the cells were washed with 200  $\mu$ L PBS<sup>-</sup>. The experimental groups were treated with the BPE at concentrations of 60  $\mu$ g/ml, 30  $\mu$ g/ml, 15  $\mu$ g/ml. The senescent group and the control group were cultured with culture medium. After 48 hours, the total RNA from the fibroblasts was extracted using the Easy-Blue Total RNA Extraction Kit (iNtRON Biotechnology).

Real-Time Reverse Transcription Quantitative PCR (Real-Time RT-qPCR)

Real-time reverse transcription quantitative PCR was

performed on the Mastercycler<sup>®</sup> ep realplex Real-Time PCR System using the Luna<sup>®</sup> Universal One-Step RT-qPCR Kit. The results are presented as the average of three separate replicates, with quantification performed by normalizing to GAPDH expression. Relative gene expression was determined using the  $\Delta\Delta C_t$  method ( $C_t$  is the threshold cycle value).

### CD90 Expression

Human fibroblasts were seeded in a 6-well plate. The cell density was  $2 \times 10^5$  cells per well (in 1 mL volume). These cells were treated with 10  $\mu$ M, 20  $\mu$ M, 30  $\mu$ M etoposide and incubated for 48 hours. Afterwards, the cells were labeled with 5  $\mu$ L CD90 (BD Biosciences, Franklin Lakes, NJ) in 100  $\mu$ L of staining buffer for 15 minutes. The cells were detected using a FACSCalibur flow cytometer. Data were analyzed using CellQuest Pro software (BD Biosciences, Franklin Lakes, NJ).

For the BPE testing, human fibroblasts ( $2 \times 10^5$  cells/well) were cultured in a 6-well plate in 1 mL of culture medium. After 24 hours, the cells were treated with 20  $\mu$ M etoposide to make a senescent fibroblast model for 48 hours. After that, the cells were washed with 200  $\mu$ L PBS<sup>-</sup>. The experimental groups were treated with the BPE at concentrations of 60  $\mu$ g/ml, 30  $\mu$ g/ml, 15  $\mu$ g/ml. The senescent group and the control group were cultured with culture medium. After 48 hours, the cells were labeled with 5  $\mu$ L CD90 (BD Biosciences, Franklin Lakes, NJ) in 100  $\mu$ L of staining buffer for 15 minutes. The cells were detected using a FACSCalibur flow cytometer. Data were analyzed using CellQuest Pro software (BD Biosciences, Franklin Lakes, NJ).

### Statistical Analysis

Data were collected and processed using GraphPad Prism 9 software. The results are presented as mean  $\pm$  SD. Differences between treatments were assessed using one-way ANOVA, with statistical significance set at  $p < 0.05$ .

## RESULTS

### The cytotoxicity of etoposide on human fibroblast cells

To evaluate the impact of etoposide on human fibroblast cells, we determined the IC<sub>50</sub> value through the Alamar Blue assay, measuring the level of cell metabolism after a 48-hour treatment with etoposide. The results show that the IC<sub>50</sub> value was found to be  $32.08 \pm 2.85 \mu$ M. Based on these data, the etoposide concentrations used for further evaluation were 10  $\mu$ M, 20  $\mu$ M, and 30  $\mu$ M (Figure 1).

**Table 1: The forward and reverse primer sequences**<sup>20-22</sup>

Gene	Primers
<i>p53</i>	F: 5'-GGTTCCGTCTGGGCTTCTT-3' R: 5'-GGGCCAGACCATCGCTATC-3'
<i>p21</i>	F: 5'-CTTCGACCTTTGTCACCGAGA-3' R: 5'-AGGTCCACATGGTCTTCCTC-3'
<i>p16</i>	F: 5'-CATAGATGCCGCGGAAGGT -3' R:5'-CTAAGTTCCCGAGGTTTCTCAGA-3'
<i>GADPH</i>	F: 5'-GAGTCCACTGGCGTCTTC-3' R: 5'-GGGGTGCTAAGCAGTTGGT-3'

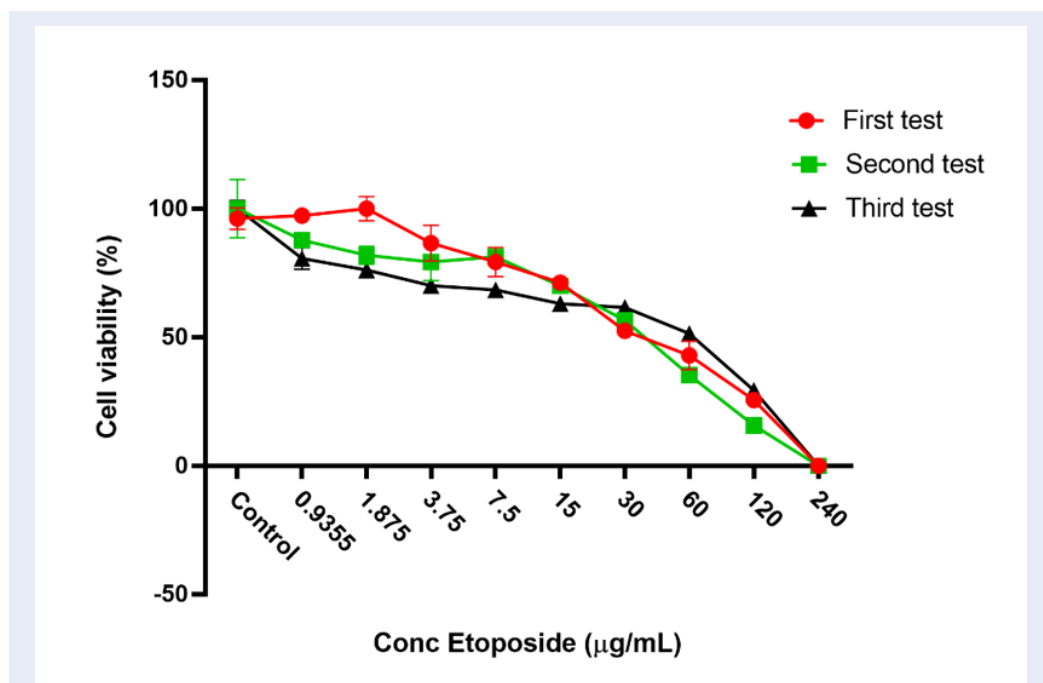


**Figure 1: The cytotoxicity of etoposide on human fibroblast cells.** hFs were treated with etoposide for 48 hours, and the cell metabolism was measured via the Alamar Blue assay. Statistical data from three replicates of the experiment were processed using GraphPad Prism 9.0 software. **Abbreviations:** conc: Concentration; hFs: human fibroblasts

**The evaluation of cell size of etoposide-induced-fibroblast**

Human fibroblasts treated with etoposide exhibited changes in morphology, becoming flattened and adopting a "fried egg" shape (Figure 2A). A few small cells remained similar in size to the control group. The mean diameter of cells after treatment with 10 µM etoposide was 24.40 µm ± 0.65 µm, which was 41.88% larger than the control group (p < 0.0001). In the group treated with 20 µM etoposide, the mean cell diameter was 24.43 µm ± 0.29 µm. This increase

was not significant compared to the 10 µM group (p > 0.05) but represented a 42.08% increase compared to the control group (p < 0.0001). In the group treated with 30 µM etoposide, the number of large cells increased, and the diameter of these cells also increased to 26.48 ± 0.20 µm, 54.26% higher than the control group (p < 0.0001). In the control group, the average diameter of the cells was about 17.35 ± 0.48 µm. These results demonstrate that treatment with etoposide at concentrations of 10 µM, 20 µM, and 30 µM led to an increase in the diameter of human fibro-

lasts in suspension compared to the control group (Figure 2 B,C). The cell shape became more flattened, changing to a "fried egg" form.

### The increase of SA- $\beta$ -Galactosidase in fibroblast induced with etoposide

After 48 hours of treatment with 10  $\mu$ M etoposide, the proportion of SA- $\beta$ -Galactosidase-positive cells was  $22.94 \pm 2.28\%$ , which was not statistically significant compared to the control group ( $p > 0.05$ ). In the 20  $\mu$ M etoposide group, this proportion was  $35.61 \pm 0.40\%$ , an increase of 1.7 times compared to the control group ( $p < 0.001$ ). A more significant increase, 2.09 times compared to the control group ( $p < 0.0005$ ), was observed in cells treated with 30  $\mu$ M etoposide, reaching  $43.48 \pm 5.05\%$ . These results indicate that SA- $\beta$ -Gal accumulation increased significantly after 48 hours of etoposide treatment at concentrations of 20  $\mu$ M and 30  $\mu$ M (Figure 3).

### The expression of p16, p21 and p53 gene in fibroblast treated with etoposide

Cell senescence is associated with increased regulation of the tumor suppressor gene and cell cycle regulators p53, p21<sup>CIP1/WAF</sup>, and p16<sup>INK4A</sup> 10. We examined the messenger RNA levels of p16, p21, and p53 to evaluate cell senescence; higher levels were found in the etoposide-treated cells. Notably, the expression of the p16, p21, and p53 genes in the 20  $\mu$ M etoposide-treated cells increased 5.6 times (\*\* $p < 0.001$ ), 2.7 times (\* $p < 0.05$ ), and 4 times (\* $p < 0.05$ ) compared to the control group (Figure 4). These results indicate that etoposide increases the expression of senescence-related genes and has the potential to induce cellular senescence.

### Positive expression of CD90

Previous studies have shown that CD90 positivity is one of the markers for identifying fibroblasts. These cells, treated with etoposide at concentrations of 10  $\mu$ M, 20  $\mu$ M, and 30  $\mu$ M, had CD90 positivity rates of 98.44%, 98.49%, and 96.79%, respectively (Figure 5). In the control group, the percentage of cells positive for the CD90 marker was 95.78% (Figure 5). Together with the morphology of the cells in culture, this result shows that the cells maintained the characteristics of fibroblasts when treated with etoposide.

The results above indicate that the concentration of etoposide at 20  $\mu$ M for 48 hours is the optimal concentration to induce the senescent fibroblast model. When treated with this concentration, fibroblasts exhibited statistically significant markers of senescent

cells compared to the normal, such as increased cell size (42.08% increase compared to the control), increased expression of SA- $\beta$ -Gal (1.7 times increase compared to the control), increased expression of p16, p53, and p21 genes, and the percentage of cells expressing CD90<sup>+</sup> increased to 98.49%.

### The cytotoxicity of BPE on fibroblasts

To determine the potential of BPE on senescent fibroblasts, we first performed a cytotoxicity test of this extract on cells using the Alamar Blue assay. The IC50 result of BPE on fibroblasts was  $212.1 \pm 5.27 \mu$ g/ml. BPE at concentrations of 60  $\mu$ g/ml, 30  $\mu$ g/ml, and 15  $\mu$ g/ml showed the best cell survival rate when applied to fibroblasts (Figure 6). Therefore, we chose these three concentrations to further test the effects of BPE on senescent fibroblasts.

### The cell size assessment of BPE treated-senescent fibroblast

Senescent cells change shape, becoming larger and flatter. Therefore, the decrease in cell diameter is one of the criteria to evaluate the potential of BPE on these senescent cells. In this experiment, senescent fibroblasts were treated with concentrations of BPE at 60  $\mu$ g/ml, 30  $\mu$ g/ml, and 15  $\mu$ g/ml. After 48 hours, the size of fibroblasts was evaluated by cell diameter (using Axio Vision v4.0 software from Carl Zeiss). When fibroblasts were exposed to the extract of *Boesenbergia pandurata*, the cell size of senescent fibroblasts was smaller than that of untreated senescent cells (Figure 7). This size was similar to the normal cell size. Specifically, at a concentration of 15  $\mu$ g/ml of BPE, fibroblast size was 27% smaller than untreated cells (about  $21.26 \mu$ m  $\pm$   $2.68 \mu$ m) ( $p < 0.05$ ). At 30  $\mu$ g/ml, the size of the cells was 1.42 times smaller than that of senescent cells ( $p < 0.005$ ). In summary, these results show that the extract of *Boesenbergia pandurata* affects the aging process by reducing cell size.

### BPE reducing the positive of SA- $\beta$ -galactosidase in senescent fibroblast

The presence of the SA- $\beta$ -Galactosidase enzyme through an X-gal staining kit at pH 6.0 is used to confirm senescent cells. In this experiment, senescent fibroblasts were treated with BPE at concentrations of 60  $\mu$ g/ml, 30  $\mu$ g/ml, and 15  $\mu$ g/ml for 48 hours to examine the effect of this extract on senescent cells. Then, the cells were stained with a Galactosidase Staining Kit (Abcam, UK), and senescent cells exhibited a blue color.



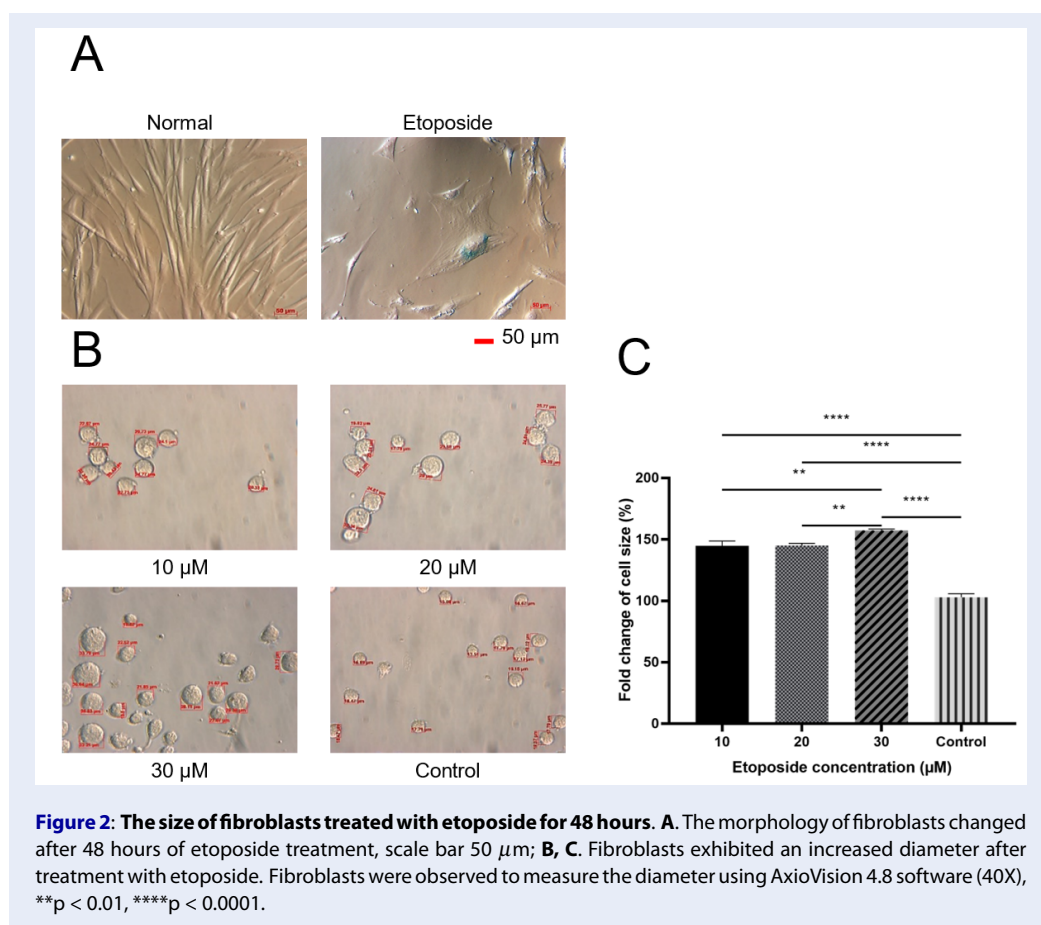


**Figure 2: The size of fibroblasts treated with etoposide for 48 hours.** **A.** The morphology of fibroblasts changed after 48 hours of etoposide treatment, scale bar 50 µm; **B, C.** Fibroblasts exhibited an increased diameter after treatment with etoposide. Fibroblasts were observed to measure the diameter using AxioVision 4.8 software (40X), \*\* $p < 0.01$ , \*\*\*\* $p < 0.0001$ .

The results show that senescent fibroblasts treated with BPE displayed a noticeable decrease in SA- $\beta$ -Galactosidase expression, which is a common marker of cellular aging. Senescent cells treated with BPE at a concentration of 15 µg/ml exhibited a 1.2-fold reduction in SA- $\beta$ -Galactosidase positivity compared to untreated cells (26.311%  $\pm$  1.177%) ( $p < 0.0001$ ). At a higher concentration of 30 µg/ml, the proportion of SA- $\beta$ -Galactosidase positive cells was 25.905%  $\pm$  0.431%, representing a 1.22-fold decrease compared to senescent cells ( $p < 0.0001$ ). At the highest concentration tested, 60 µg/ml, the SA- $\beta$ -Galactosidase positivity rate was 27.735%  $\pm$  1.093%, which is a 1.14-fold reduction compared to senescent cells ( $p < 0.001$ ).

#### BPE reducing p16, p53, p21 gene expression

To evaluate the potential of the BP extract on senescent cells, the decrease in aging-related genes illustrates these effects<sup>9</sup>. The results show that treating senescent cells with BPE decreases the expression of genes *p16*, *p21*, and *p53*, in contrast to untreated senescent cells (Figure 9). Senescent cells treated with

BPE demonstrate a reduction in p16 gene expression by 5.89 times ( $p < 0.0001$ ), 21.3 times ( $p < 0.0001$ ), and 18.85 times ( $p < 0.0001$ ) at concentrations of 15 µg/ml, 30 µg/ml, and 60 µg/ml, respectively, compared with the senescent group. Similarly, BP-treated senescent fibroblasts at concentrations of 15 µg/ml, 30 µg/ml, and 60 µg/ml also reduced p21 and p53 gene expressions by 5.68 times ( $p < 0.001$ ), 6.74 times ( $p < 0.001$ ), and 3.79 times ( $p < 0.001$ ) for the former gene, and by 3.26 times ( $p < 0.001$ ), 5 times ( $p < 0.0001$ ), and 2.73 times ( $p < 0.001$ ) for the latter gene, respectively, compared to the senescent group.

#### The positive expression with CD90

The results indicate that cells expressing the CD90 marker were positive in both the extract-treated and control groups (Figure 10). In the control group, the highest proportion of cells positive for the CD90 marker was 98.76%. This was followed by senescent cells with a CD90 positivity rate of 98.71%. Senescent cells treated with BPE also exhibited high CD90 expression (above 98%).

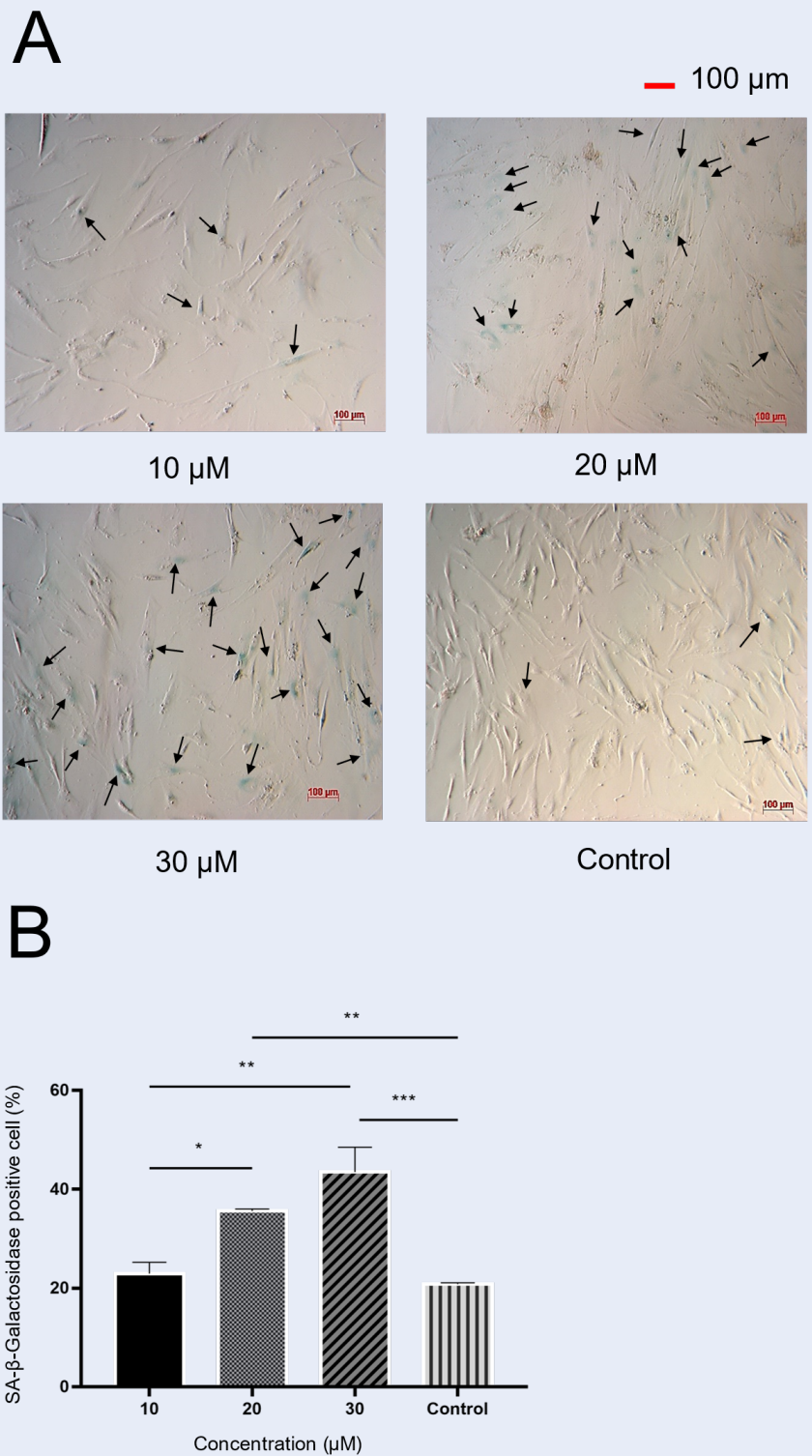


**Figure 3: Etoposide increased the proportion of SA-β-Galactosidase-positive cells in human fibroblasts. A.** Morphology of human fibroblasts, scale bar 100 μm; **B.** The proportion of SA-β-Galactosidase-positive cells in human fibroblasts exposed to etoposide after 48 hours, \*p < 0.05, \*\*p < 0.01, \*\*\* p < 0.001. SA-β-Galactosidase: Senescence-associated beta-galactosidase.

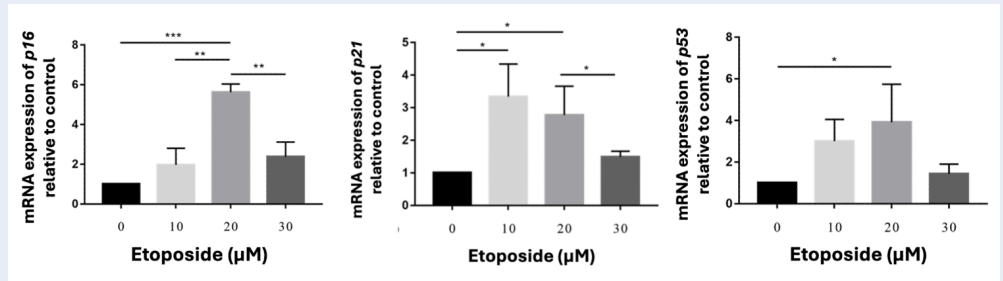


**Figure 4: Gene expression comparison between etoposide-treated cells and normal cells.** Cells were induced with etoposide at concentrations of 10  $\mu\text{M}$ , 20  $\mu\text{M}$ , and 30  $\mu\text{M}$  for 48 hours, and the mRNA expression of p16, p21, and p53 was measured by RT-qPCR. The relative expression ( $\Delta\Delta\text{Ct}$ ) of the three genes was analyzed, and GAPDH served as an internal reference gene. \* $p < 0.05$ , \*\* $p < 0.01$ , \*\*\* $p < 0.001$ .

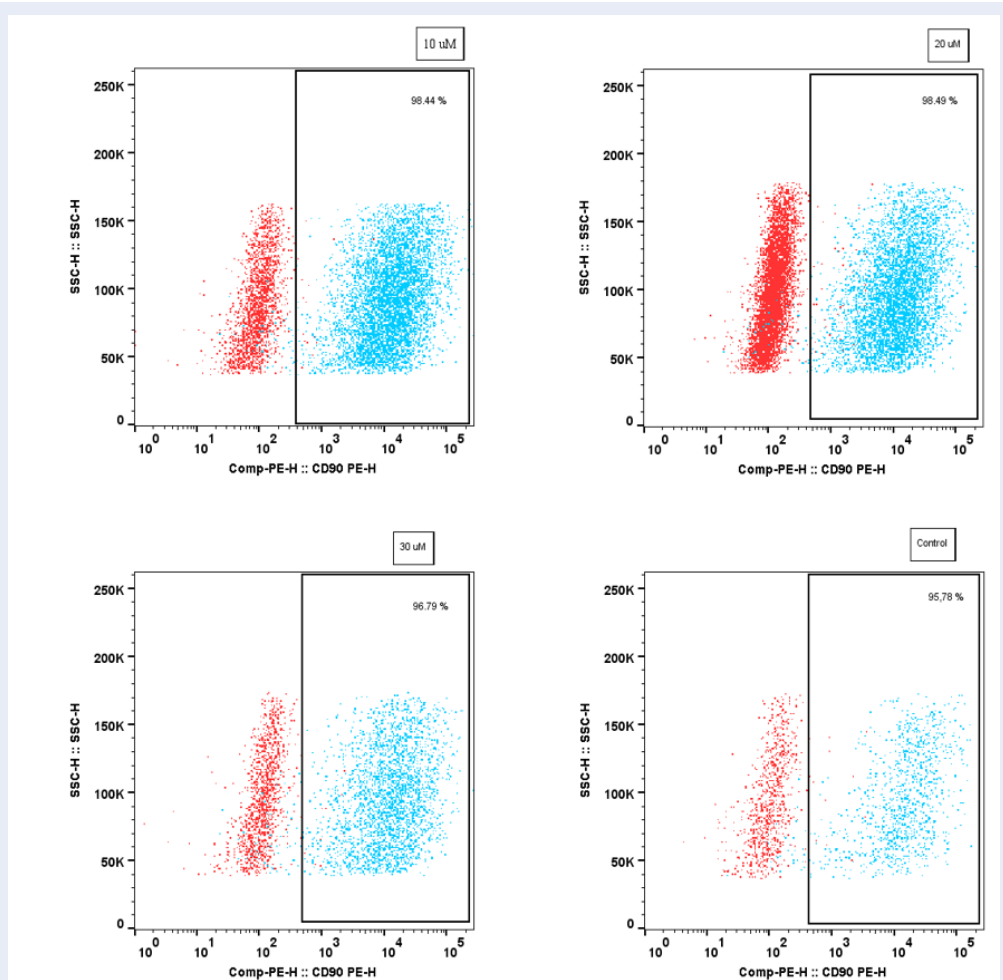


**Figure 5: Etoposide-treated fibroblasts CD90 positive.** Fibroblasts were cultured in 6-well plates at a density of 200,000 cells per well. After 48 hours of treatment with etoposide at concentrations of 10  $\mu\text{M}$ , 20  $\mu\text{M}$ , 30  $\mu\text{M}$ , and control, cells were stained with a CD90 marker. Results were obtained using a FACSMelody machine and analyzed using FlowJo software. Blue represents cells expressing CD90<sup>+</sup>, and red represents cells without staining.



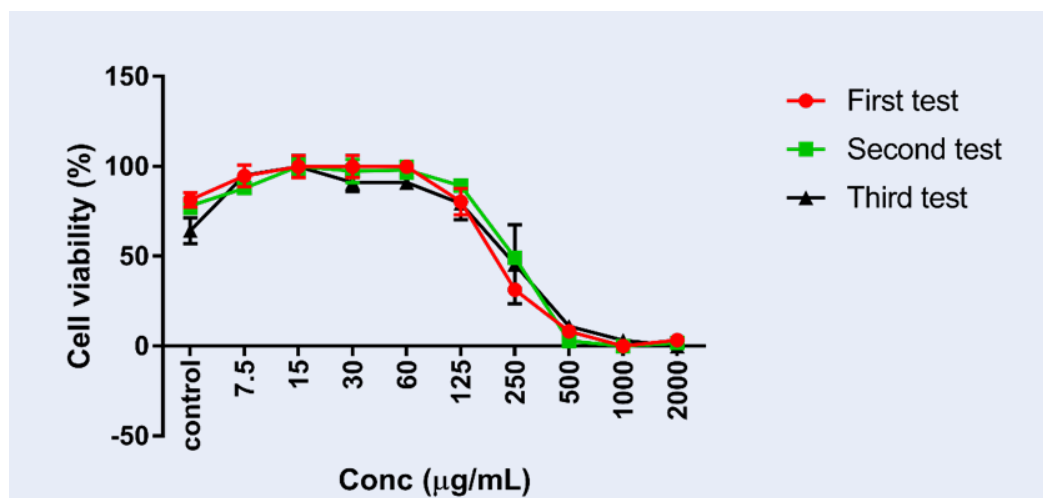


**Figure 6: The proliferation curve of BPE-treated fibroblasts.** hFs were treated with BPE for 48 hours, and the metabolism of cells was measured via the Alamar Blue assay. Statistical data from three replicates of the experiment were processed using Graph Prism 9.0 software.

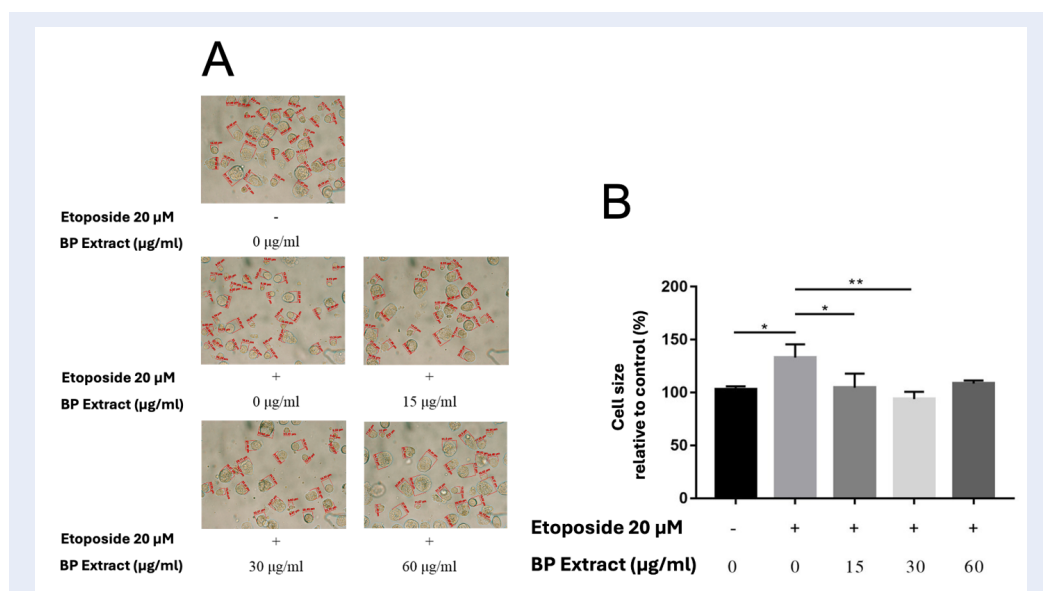


**Figure 7: BPE reduced the size of senescent fibroblasts.** **A.** Morphology of human fibroblasts exposed to BPE. Senescent fibroblasts were cultured in a 48-well plate (5,000 cells/well). After 48 hours of treatment with BPE, suspension cell diameters were measured using Axio Vision v4.0 software. **Abbreviations:** BPE: *Boesenbergia pandurata* extract; Magnification 200X. "+": aging cells, "-": normal cells; **B.** The relative cell size; the cell diameter of the control group was converted to 100% to compare the increase in cell size. "+": senescent cells, "-": normal cells. \*p < 0.05, \*\*p < 0.01.

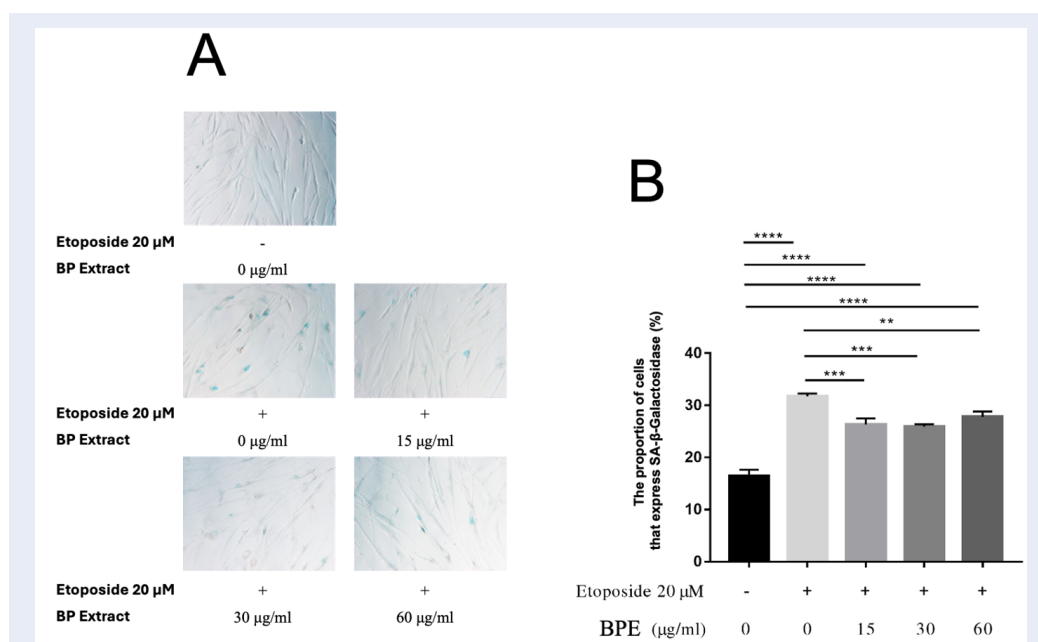


**Figure 8: BPE decreased the proportion of SA-β-Galactosidase positive senescent fibroblasts.** A. Morphology of human fibroblasts, magnification 200X; B. The proportion of SA-β-Galactosidase positive senescent fibroblasts exposed to BPE after 48 hours. **Abbreviations:** SA-β-Galactosidase: Senescence-associated beta-galactosidase, BPE: *Boesenbergia Pandurata* extract; \*p < 0.05, \*\*p < 0.01, \*\*\*p < 0.001, \*\*\*\*p < 0.0001.

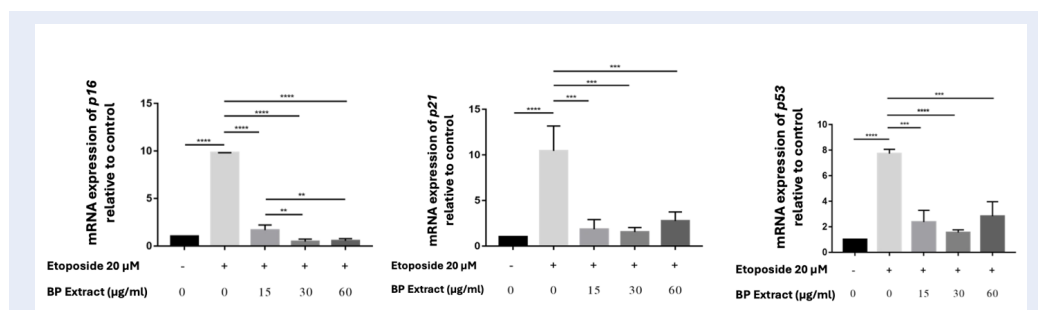


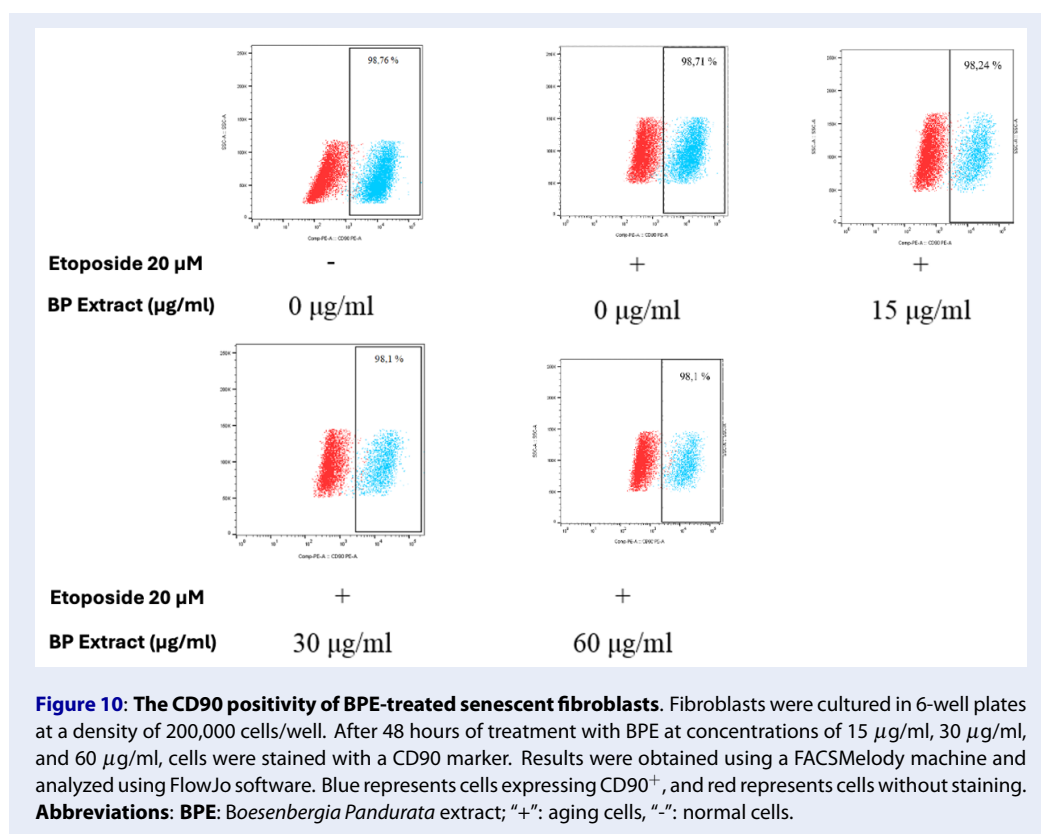
**Figure 9: Reducing gene expression in BPE-treated cells compared with the senescent group.** Senescent cells were treated with BPE at 15 μg/ml, 30 μg/ml, and 60 μg/ml for 48 hours, and the mRNA expression of p16, p21, and p53 was measured by RT-qPCR. The relative expression (-ΔΔCt) of the three genes was analyzed, with GAPDH serving as an internal reference gene. **Abbreviations:** BPE: *Boesenbergia Pandurata* extract; "+": aging cells, "-": normal cells \*p < 0.05, \*\*p < 0.01, \*\*\*p < 0.001, \*\*\*\*p < 0.0001.

## DISCUSSION

Aging is a complex process caused by both intrinsic and extrinsic factors<sup>8</sup>. Lozoptin *et al.* updated the twelve hallmarks of aging, which include genomic instability, telomere attrition, epigenetic alterations, loss of proteostasis, disabled macroautophagy, deregulated nutrient-sensing, mitochondrial dysfunction, cellular senescence, stem cell exhaustion, altered intercellular communication, chronic inflammation, and dysbiosis<sup>3</sup>. Notably, studies have shown that ex-

periments targeting one of these hallmarks can have a direct impact on the overall aging process<sup>23</sup>. Therefore, research aimed at improving the cellular aging process represents a promising direction in anti-aging and rejuvenation therapies.

Numerous cosmetic approaches have been explored to address social demands, with natural extracts gaining prominence due to their safety profiles and compatibility with diverse skin types<sup>24</sup>. Although the potential of *Boesenbergia Pandurata* has been primarily investigated in the context of its anti-cancer proper-



ties, such as in liver and pancreatic cancers, its anti-aging potential remains underexplored<sup>18</sup>. Moreover, developing a senescent cell model is crucial for assessing the efficacy of novel therapeutic strategies in this domain.

Etoposide has been identified as an agent capable of inducing cellular senescence at low concentrations due to its inhibition of topoisomerase and induction of DNA double-strand breaks (DSBs)<sup>25</sup>. This study demonstrated that etoposide induces senescence in human fibroblasts at a concentration of 20  $\mu\text{M}$ . This finding is consistent with previous studies showing that low concentrations of etoposide induce senescence in other cell lines, such as the H29SR adrenocortical cell line<sup>26</sup>, the HepG2 hepatoblastoma cell line<sup>17</sup>, and the A549 lung cancer cell line<sup>27</sup>. At this concentration, human fibroblasts exhibited a 41.88% increase in cell size compared to the control group ( $p < 0.0001$ ). This cell enlargement has also been reported in the work of Anna Litwiniec *et al.* (2018), which showed that low-dose etoposide treatment induces cell size increase, chromatin condensation, segmented or lobulated nuclei, and multinucleation in treated cells<sup>26</sup>, and Tigges *et al.* (2014), who reported increased cell size and diminished prolifera-

tive capacity following etoposide treatment<sup>1</sup>. Additionally, this study indicates that fibroblasts treated with 20  $\mu\text{M}$  etoposide exhibited a 35.61% increase in SA- $\beta$ -Gal expression, a well-known marker of senescence, compared to the control group. In a related study, Taiki Nagano (2016) claimed a significant increase in SA- $\beta$ -Gal expression in HepG2 cells treated with 10  $\mu\text{M}$  etoposide<sup>17</sup>, further supporting the role of etoposide in promoting senescence markers across different cell types. In the senescent state, senescence-inducing factors converge on tumor suppressor pathways, specifically the p53/p21CIP1 and p16INK4A/pRB pathways, resulting in cell cycle arrest<sup>12</sup>. Our study demonstrated an increase in mRNA expression levels of the *p16*, *p53*, and *p21* genes, consistent with findings by Carlos Anerillas (2022), who reported elevated p16 expression in WI-38 cells treated with 50  $\mu\text{M}$  etoposide and in BJ fibroblasts treated with 25  $\mu\text{M}$  etoposide<sup>28</sup>. Notably, this senescent fibroblast model has been repeatedly used to test the activity of BPE and consistently shows that the signs of cellular senescence remain unchanged in the senescent group after 48 hours of testing, indicating the stability of the *in vitro* fibroblast aging model.

*Boesenbergia Pandurata* has been identified as a plant rich in phenolics, terpenoids, and flavonoids<sup>29,30</sup>,

which are known for their anti-inflammatory and antioxidant properties<sup>31-33</sup>. *In vivo* studies by Sungkyung Kim *et al.* (2012) demonstrated that the extract effectively mitigates UVB-induced skin aging in hairless mice, underscoring its potential anti-aging benefits<sup>34</sup>. Furthermore, Kim *et al.* observed significant improvements in skin hydration, gloss, and reduction in wrinkling in test subjects treated with BPE<sup>35</sup>. Do Un Kim *et al.* (2017) showed that BPE has potential as a nutraceutical or nutricosmetic ingredient, enhancing skin hydration, gloss, and reducing wrinkles when administered orally, with the ethanol extract containing 8% panduratin A<sup>36</sup>. While these results underscore the plant's promise, there is still limited research on its *in vitro* effects on cellular aging. Thus, our study aims to assess the impact of BPE on the aging process, specifically targeting its effects on senescent fibroblasts.

Our study found that the IC<sub>50</sub> of BP ethanol extract on fibroblast is 212.1 ± 5.27 µg/ml, with noteworthy observations that at concentrations of 15 µg/ml, 30 µg/ml, and 60 µg/ml, the highest percentage of viable cells was observed. Therefore, the efficacy of *Boesenbergia Pandurata* ethanol extract was assessed using an etoposide-induced cellular senescence model at these concentrations.

However, testing these concentrations on senescent fibroblasts, based on previous experiments, did not show significant differences. Therefore, even the lowest concentration in this study, 15 µg/ml, demonstrated positive effects in mitigating the aging process. The study shows that BPE at 15 µg/ml has the potential to improve the signs of cellular senescence while remaining safe for cells. This result aligns with the study of Ruttanapattanakul, J., *et al.* (2021), which found that BPE at 15.6 µg/mL (and lower) did not affect the cell viability of HaCaT cells cultured in complete media or serum-free media, after 24 hours on scratch wound closure<sup>37</sup>.

The ethanol extract of *Boesenbergia pandurata* at a concentration of 15 µg/ml reduced the size of senescent cells by 27% compared to untreated cells (approximately 21.26 µm ± 2.68 µm) (p < 0.05). A hallmark of cellular aging, the accumulation of SA-β-Gal in cellular lysosomes, was also assessed to evaluate the anti-aging potential of this extract<sup>12</sup>. The results showed a 1.2-fold reduction in SA-β-Galactosidase-positive cells relative to untreated cells (26.311% ± 1.177%) (p < 0.0001). This study further demonstrated that BPE reduces the expression of genes associated with cell cycle arrest, such as *p16*, *p53*, and *p21*. When senescent fibroblasts were induced by etoposide, these genes were upregulated compared

to normal cells; however, upon treating the senescent cells with 15 µg/ml of the extract, gene expression levels decreased. These findings align with previous studies showing BPE possesses antioxidant and anticancer properties<sup>16,29,30,32,37,38</sup>. Several studies have also reported the extract's potential in reducing UV-induced cellular aging. Compounds such as panduratin A and 4-hydroxypanduratin A, as well as the BPE, exhibit protective anti-aging effects on human skin fibroblasts against UV radiation<sup>30</sup>, reducing UV-induced MMP-1 expression by deactivating MAPK signaling pathways (ERK, p38, and JNK), which subsequently decreases cFos and c-Jun phosphorylation, leading to reduced AP-1 DNA binding activity<sup>39</sup>. The extract's anti-inflammatory potential may also contribute to mitigating aging processes, although this was not examined in the current study<sup>39,40</sup>. Overall, based on these preliminary findings with the ethanol extract of *B. pandurata*, it can be concluded that the extract is effective in alleviating cellular aging processes through several characteristic biomarkers.

## CONCLUSIONS

This study successfully established a senescent fibroblast model using the etoposide agent. The optimal etoposide concentration for inducing fibroblast senescence was determined to be 20 µM, with a treatment duration of 48 hours. The IC<sub>50</sub> of etoposide for fibroblasts is 32.08 µM ± 2.854 µM. Furthermore, this study demonstrated the potential of the ethanol extract of *Boesenbergia pandurata* root in modulating specific senescence characteristics induced by etoposide. The extract showed an IC<sub>50</sub> for fibroblast inhibition of 212.1 µg/ml ± 5.27 µg/ml. When applied at 15 µg/ml, *B. pandurata* extract improved several markers of cellular aging, including reduced cell size, decreased SA-β-Galactosidase activity, and downregulated expression of p16, p53, and p21.

## ABBREVIATIONS

**BPE** - Boesenbergia Pandurata Extract, **CD90** - Cluster of Differentiation 90, **FBS** - Fetal Bovine Serum, **GAPDH** - Glyceraldehyde 3-phosphate dehydrogenase, **hFs** - human fibroblasts, **IC<sub>50</sub>** - Half-maximal inhibitory concentration, **µM** - Micromolar, **µg/ml** - Micrograms per milliliter, **mRNA** - Messenger RNA, **PBS** - Phosphate Buffered Saline, **pH** - Potential Hydrogen, **PCR** - Polymerase Chain Reaction, **pRB** - Retinoblastoma Protein, **p16<sup>INK4A</sup>** - p16 Inhibitor of Cyclin-dependent Kinase 4A, **p21<sup>CIP1</sup>** - p21 Cyclin-dependent Kinase Inhibitor 1, **p53** - Tumor protein p53, **qPCR** - Quantitative Polymerase Chain Reaction, **SA-β-Gal** - Senescence-associated

beta-Galactosidase, **SASP** - Senescence-associated secretory phenotype, **UVB** - Ultraviolet B

## ACKNOWLEDGMENTS

I would like to express my sincere gratitude to Assoc. Prof. Dr. Phuc Van Pham, thank you for your technical support throughout this project. His expertise and guidance have been crucial in overcoming challenges and achieving the research goals.

## AUTHOR'S CONTRIBUTIONS

Phuc Hong Vo performed the experiments, analyzed the results, and wrote the manuscript. Nghia Minh Do supports the identification and verification of *Boesenbergia pandurata*. Sinh Truong Nguyen supervised the research and reviewed the manuscript. All authors read and approved the final manuscript.

## FUNDING

This study was granted by Stem Cell Institute, University of Science, Viet Nam National University Ho Chi Minh City, Viet Nam.

## AVAILABILITY OF DATA AND MATERIALS

Data and materials used and/or analyzed during the current study are available from the corresponding author on reasonable request.

## ETHICS APPROVAL AND CONSENT TO PARTICIPATE

Not applicable.

## CONSENT FOR PUBLICATION

Not applicable.

## COMPETING INTERESTS

The authors declare that they have no competing interests.

## REFERENCES

1. Tigges J, Krutmann J, Fritsche E, Haendeler J, Schaal H, Fischer JW, et al. The hallmarks of fibroblast ageing. *Mechanisms of ageing and development*. 2014;138:26–44. Available from: <https://doi.org/10.1016/j.mad.2014.03.004>.
2. López-Otín C, Blasco MA, Partridge L, Serrano M, Kroemer G, et al. The hallmarks of aging. *Cell*. 2013;153(6):1194–217. Available from: <https://doi.org/10.1016/j.cell.2013.05.039>.
3. López-Otín C, Blasco MA, Partridge L, Serrano M, Kroemer G. Hallmarks of aging: an expanding universe. *Cell*. 2023;186(2):243–78. PMID: 36599349. Available from: <https://doi.org/10.1016/j.cell.2022.11.001>.
4. Cavinato M, Wedel S, Jansen-Dürr P. Aging of Cells In Vitro. *Reference Module in Biomedical Sciences*. 2020;2020:138–48. Available from: <https://doi.org/10.1016/B978-0-12-801238-3.11409-6>.
5. Veronesi F, Contartese D, Sarno LD, Borsari V, Fini M, Giavarsi G. In Vitro Models of Cell Senescence: A Systematic Review on Musculoskeletal Tissues and Cells. *International Journal of Molecular Sciences*. 2023;24(21):15617. PMID: 37958603. Available from: <https://doi.org/10.3390/ijms242115617>.
6. Kirkland JL, Tchkonja T. Cellular Senescence: A Translational Perspective. *EBioMedicine*. 2017;21:21–8. PMID: 28416161. Available from: <https://doi.org/10.1016/j.ebiom.2017.04.013>.
7. Wyles SP, Tchkonja T, Kirkland JL. Targeting Cellular Senescence for Age-Related Diseases: Path to Clinical Translation. *Plastic and Reconstructive Surgery*. 2022;150:20–6. PMID: 36170432. Available from: <https://doi.org/10.1097/PRS.0000000000009669>.
8. Kumari R, Jat P. Mechanisms of cellular senescence: cell cycle arrest and senescence associated secretory phenotype. *Frontiers in Cell and Developmental Biology*. 2021;9:645593. PMID: 33855023. Available from: <https://doi.org/10.3389/fcell.2021.645593>.
9. Micco RD, Krizhanovsky V, Baker D, d'Adda di Fagagna F. Cellular senescence in ageing: from mechanisms to therapeutic opportunities. *Nature Reviews Molecular Cell Biology*. 2021;22(2):75–95. PMID: 33328614. Available from: <https://doi.org/10.1038/s41580-020-00314-w>.
10. Muñoz-Espín D, Serrano M. Cellular senescence: from physiology to pathology. *Nature Reviews Molecular Cell Biology*. 2014;15(7):482–96. PMID: 24954210. Available from: <https://doi.org/10.1038/nrm3823>.
11. Valieva Y, Ivanova E, Fayzullin A, Kurkov A, Igrunkova A. Senescence-Associated  $\beta$ -Galactosidase Detection in Pathology. *Diagnostics (Basel)*. 2022;12(10):2309. PMID: 36291998. Available from: <https://doi.org/10.3390/diagnostics12102309>.
12. Wang AS, i G Dreesen OJF. Biomarkers of cellular senescence and skin aging. *Frontiers in genetics*. 2018;9:247. Available from: <https://doi.org/10.3389/fgene.2018.00247>.
13. Lee BY, Han JA, Im JS, Morrone A, Johung K, Goodwin EC. Senescence-associated  $\beta$ -galactosidase is lysosomal  $\beta$ -galactosidase. *Aging Cell*. 2006;5(2):187–95. PMID: 16626397. Available from: <https://doi.org/10.1111/j.1474-9726.2006.00199.x>.
14. Lawrence M, Goyal A, Pathak S, Ganguly P. Cellular Senescence and Inflammaging in the Bone: Pathways, Genetics, Anti-Aging Strategies and Interventions. *International Journal of Molecular Sciences*. 2024;25(13):7411. PMID: 39000517. Available from: <https://doi.org/10.3390/ijms25137411>.
15. Dimri GP, et al. A biomarker that identifies senescent human cells in culture and in aging skin in vivo. *Proc Natl Acad Sci USA*. 1995;92:9363–7. Available from: <https://doi.org/10.1073/pnas.92.20.9363>.
16. Eng-Chong T, L YK, C CF, H CH, and Li-Ping CT SMW, F GT, et al. *Boesenbergia rotunda*: from ethnomedicine to drug discovery. *Evidence - Based Complementary and Alternative Medicine*. 2012;2012(1):473637. Available from: <https://doi.org/10.1155/2012/473637>.
17. Nagano T, Nakano M, Nakashima A, Onishi K, Yamao S, Enari M. Identification of cellular senescence-specific genes by comparative transcriptomics. *Scientific Reports*. 2016;6(1):31758. PMID: 27545311. Available from: <https://doi.org/10.1038/srep31758>.
18. Nguyen ST, et al. Isopanduratin A isolated from *Boesenbergia pandurata* reduces HepG2 hepatocellular carcinoma cell proliferation in both monolayer and three-dimensional cultures. *InCancer Biology and Advances in Treatment Springer International Publishing*. 2020;p. 131–143. Available from: [https://doi.org/10.1007/5584\\_2020\\_523](https://doi.org/10.1007/5584_2020_523).
19. Nguyen MT, Nguyen HX, Dang PH, Le TH, Do TN, Omar AM, et al. Panduratinins Q-Y, dimeric metabolites from *Boesenbergia rotunda* and their antiausterity activities against the PANC-1 human pancreatic cancer cell line. *Phytochemistry*. 2021;183:112646. PMID: 33421887. Available from: <https://doi.org/10.1016/j.phytochem.2020.112646>.
20. Ando K, Nakamura Y, Nagase H, Nakagawara A, Koshinaga T, Wada S. Co-Inhibition of the DNA Damage Response



- and CHK1 Enhances Apoptosis of Neuroblastoma Cells. *International Journal of Molecular Sciences*. 2019;20(15):3700. PMID: 31362335. Available from: <https://doi.org/10.3390/ijms20153700>.
21. Siu MK, Yeung MC, Zhang H, Kong DS, Ho JW, Ngan HY. p21-Activated kinase-1 promotes aggressive phenotype, cell proliferation, and invasion in gestational trophoblastic disease. *American Journal of Pathology*. 2010;176(6):3015–22. PMID: 20413688. Available from: <https://doi.org/10.2353/ajpath.2010.091263>.
  22. Al-Khalaf HH, Ghebeh H, Inass R, Aboussekhra A. Senescent Breast Luminal Cells Promote Carcinogenesis through Interleukin-8-Dependent Activation of Stromal Fibroblasts. *Molecular and Cellular Biology*. 2019;39(2):e00359–18. PMID: 30397077. Available from: <https://doi.org/10.1128/MCB.00359-18>.
  23. Chaib S, Tchkonja T, Kirkland JL. Cellular senescence and senolytics: the path to the clinic. *Nature Medicine*. 2022;28(8):1556–68. PMID: 35953721. Available from: <https://doi.org/10.1038/s41591-022-01923-y>.
  24. Xie M, Jiang Z, Lin X, Wei X, et al. Application of plant extracts cosmetics in the field of anti-aging. *Journal of Dermatologic Science and Cosmetic Technology*. 2024;2024:100014. Available from: <https://doi.org/10.1016/j.jdsct.2024.100014>.
  25. Li Z, Sun B, Clewell RA, Adeleye Y, Andersen ME, Zhang Q, et al. Dose-response modeling of etoposide-induced DNA damage response. *Toxicological sciences*. 2014;137(2):371–84. Available from: <https://doi.org/10.1093/toxsci/kit259>.
  26. Tamamori-Adachi M, Koga A, Susa T, Fujii H, Tsuchiya M, Okinaga H. DNA damage response induced by Etoposide promotes steroidogenesis via GADD45A in cultured adrenal cells. *Scientific Reports*. 2018;8(1):9636. PMID: 29941883. Available from: <https://doi.org/10.1038/s41598-018-27938-5>.
  27. Litwiniec A, Gackowska L, Helmin-Basa A, Zuryń A, Grzanka A. Low-dose etoposide-treatment induces endoreplication and cell death accompanied by cytoskeletal alterations in A549 cells: does the response involve senescence? The possible role of vimentin. *Cancer Cell International*. 2013;13(1):9. PMID: 23383739. Available from: <https://doi.org/10.1186/1475-2867-13-9>.
  28. Anerillas C, Herman AB, Rossi M, Munk R, Lehrmann E, Martindale JL, et al. Early SRC activation skews cell fate from apoptosis to senescence. *Science Advances*. 2022;8(14):eabm0756. PMID: 35394839. Available from: <https://doi.org/10.1126/sciadv.abm0756>.
  29. Hop NQ, Son NT. *Boesenbergia rotunda* (L.) Mansf.: A review of phytochemistry, pharmacology, and pharmacokinetics. *Current Organic Chemistry*. 2023;27(21):1842–56. Available from: <https://doi.org/10.2174/0113852728278058231123094250>.
  30. Chahyadi A, Hartati R, Wirasutisna KR, Elfahmi. *Boesenbergia pandurata* Roxb., an Indonesian medicinal plant: Phytochemistry, biological activity, plant biotechnology. *Procedia Chemistry*. 2014;13:13–37. Available from: <https://doi.org/10.1016/j.proche.2014.12.003>.
  31. Sujana D, Sumiwi SA, Saptarini NM, Levita J. The Nephroprotective Activity of *Boesenbergia Rotunda* Rhizome by Reducing Creatinine, Urea Nitrogen, Glutamic Pyruvic Transaminase, and Malondialdehyde Levels in the Blood and Attenuating the Expression of Hmcr1 (KIM-1), Lcn2 (NGAL), Casp3, and Casp7 Genes in the Kidney Cortex of Cisplatin-Induced Sprague-Dawley Rats. *Journal of Experimental Pharmacology*. 2024;16:189–200. PMID: 38736464. Available from: <https://doi.org/10.2147/JEP.S459483>.
  32. Thongrong S, Promsrisuk T, Sriraksa N, Surapinit S, Jittiwat J, Kongsui R. Alleviative effect of scopolamine- induced memory deficit via enhancing antioxidant and cholinergic function in rats by pinostrobin from *Boesenbergia rotunda* (L.). *Biomedical Reports*. 2024;21(3):130. PMID: 39070112. Available from: <https://doi.org/10.3892/br.2024.1818>.
  33. Sritananuwat P, Samseethong T, Jitsaeng K, Duangjit S, Opanasopit P, Rangsimawong W. Effectiveness and Safety of *Boesenbergia rotunda* Extract on 3T3-L1 Preadipocytes and Its Use in Capsaicin-Loaded Body-Firming Formulation: In Vitro Biological Study and In Vivo Human Study. *Cosmetics*. 2024;11(1):24. Available from: <https://doi.org/10.3390/cosmetics11010024>.
  34. Kim S, Oh HI, Hwang JK. Oral administration of finger-root (*Boesenbergia pandurata*) extract reduces ultraviolet b-induced skin aging in hairless mice. *Food Science and Biotechnology*. 2012;21(6):1753–60. Available from: <https://doi.org/10.1007/s10068-012-0233-8>.
  35. Kim DU, Chung HC, Kim C, Hwang JK. Oral intake of *Boesenbergia pandurata* extract improves skin hydration, gloss, and wrinkling: A randomized, double-blind, and placebo-controlled study. *Journal of Cosmetic Dermatology*. 2017;16(4):512–9. PMID: 28421656. Available from: <https://doi.org/10.1111/jocd.12343>.
  36. Kim DU, Chung HC, Kim C, Hwang JK. Oral intake of *Boesenbergia pandurata* extract improves skin hydration, gloss, and wrinkling: A randomized, double-blind, and placebo-controlled study. *Journal of Cosmetic Dermatology*. 2017;16(4):512–9. PMID: 28421656. Available from: <https://doi.org/10.1111/jocd.12343>.
  37. Ruttanapattanakul J, Wikan N, Okonogi S, Takuathung MN, Buacheen P, Pitchakarn P, et al. *Boesenbergia rotunda* extract accelerates human keratinocyte proliferation through activating ERK1/2 and PI3K/Akt kinases. *Biomedicine and Pharmacotherapy*. 2021;133:111002. PMID: 33212374. Available from: <https://doi.org/10.1016/j.biopha.2020.111002>.
  38. Nguyen NT, Nguyen MT, Nguyen HX, Dang PH, Dibwe DF, Es-umi H. Constituents of the Rhizomes of *Boesenbergia pandurata* and Their Antiausterity Activities against the PANC-1 Human Pancreatic Cancer Line. *Journal of Natural Products*. 2017;80(1):141–8. PMID: 28099006. Available from: <https://doi.org/10.1021/acs.jnatprod.6b00784>.
  39. Shim JS, Han YS, Hwang JK. The effect of 4-hydroxypanduratin A on the mitogen-activated protein kinase-dependent activation of matrix metalloproteinase-1 expression in human skin fibroblasts. *Journal of Dermatological Science*. 2009;53(2):129–34. PMID: 19054653. Available from: <https://doi.org/10.1016/j.jdermsci.2008.09.002>.
  40. Isa NM, Abdelwahab SI, Mohan S, Abdul AB, Sukari MA, Taha MM. In vitro anti-inflammatory, cytotoxic and antioxidant activities of boesenbergin A, a chalcone isolated from *Boesenbergia rotunda* (L.) (fingerroot). *Brazilian Journal of Medical and Biological Research*. 2012;45(6):524–30. PMID: 22358425. Available from: <https://doi.org/10.1590/S0100-879X2012007500022>.